Molecular Structures of Ge(tpp)(OAc)$_2$ and In(tpp)(OAc) and Their Implications: Correlations between the ^{13}C NMR Chemical Shift of the Acetato Ligand and Different Types of Carboxylate Coordination in M(por)(OAc)$_n$ {por = tpp (5,10,15,20-Tetraphenylporphyrinate), tmpp (5,10,15,20-Tetrakis(4-methoxyphenyl)porphyrinate), tpyp (5,10,15,20-Tetrakis(4-pyridyl)porphyrinate); M = Ga, In, Tl, Ge, Sn; *n* = 1, 2}

Shwu-Juian Lin, Tay-Ning Hong, Jo-Yu Tung, and Jyh-Horung Chen*

Department of Chemistry, National Chung-Hsing University, Taichung 40227, Taiwan, ROC

Received October 31, 1996[⊗]

In this work, we determine the crystal structure of bis(acetato)(*meso*-tetraphenylporphyrinato)germanium(III), Ge(tpp)(OAc)$_2$. Experimental results indicate that the germanium atom has an octahedral coordination geometry. The geometry around the germanium center of the Ge(tpp)(OAc)$_2$ molecule has Ge−O(1) = 1.874(5) Å and an average Ge−N = 1.999 Å. The acetate groups are unidentately coordinated to the germanium(IV) atom. In the title compound, (acetato)(*meso*-tetraphenylporphyrinato)indium(III), In(tpp)(OAc), the coordination sphere of the In^{3+} ion is an approximately square-based pyramid in which the apical site is occupied by an asymmetric (chelating) bidentate OAc^- group. The average In−N bond distance is 2.173(3) Å, and the In atom is displaced 0.762 Å from the porphyrin plane. The In−O(1) and In−O(2) distances are 2.322(4) and 2.215(4) Å, respectively. To develop the correlations between the ^{13}C chemical shifts of the acetato ligand and types of carboxylate coordination, this work also thoroughly examines the ^{13}C NMR data of the methyl and carbonyl carbons on 13 acetato porphyrinato metal complexes M(por)(OAc)$_n$ with n = 1, 2, por = tpp, tmpp (5,10,15,20-tetrakis(4-methoxyphenyl)-porphyrinate), tpyp (5,10,15,20-tetrakis(4-pyridyl)porphyrinate), and M = Ga, In, Tl, Ge, Sn. According to these results, the ^{13}C methyl and carbonyl chemical shifts of the acetato group at 24 °C are separately located at 20.5 ± 0.2 and 168.2 ± 1.7 ppm for the acetate, which is unidentately coordinated to the metal (*i.e.*, the unidentate case) and at 18.0 ± 0.7 and 175.2 ± 1.6 ppm for the chelating bidentate case.

Introduction

In pioneering work, Kenney *et al.*[1] synthesized and characterized germanium(IV) *meso*-tetraphenylporphyrin complexes. According to their results, bis(acetato)(*meso*-tetraphenylporphyrinato)germanium(IV), Ge(tpp)(OAc)$_2$ (**9**), is a complex with and O-bound ligand. However, owing to its hydrolytic instability, the structure of Ge(tpp)(OAc)$_2$ (**9**) has not been completely characterized. Another work reported the IR and ^{1}H NMR characterization of (acetato)(*meso*-tetraphenylporphyrinato)-indium(III), In(tpp)(OAc) (**6**).[2] They noted that the value of the frequency difference $\Delta\nu$ = 141 cm^{-1} between the asymmetric and symmetric C−O vibration for In(tpp)(OAc) (**6**) excluded monoligation. Nevertheless, distinguishing between a bisligated or a dimeric mono- or dibridged complex was impossible. Apparently, more spectroscopic data would be necessary to resolve the acetato group's binding type in In(tpp)(OAc) (**6**). Details of the synthetic work can be found elsewhere.[3] Herein, we determine the structure of In(tpp)(OAc) (**6**), as derived from X-ray diffraction. In addition, X-ray diffraction, IR and ^{13}C NMR spectroscopic studies of Ge(tpp)-(OAc)$_2$ (**9**) verify that the acetate group is unidentately coordinated to the Ge atom.

A carboxylate ion, RCO_2^-, can be coordinated to a metal in one of the modes shown in Chart 1.[4] The most common forms are unidentate (**I**), chelating bidentate (**II**), free carboxylate (**V**), and bridging complexes (**III**, **IV**). Deacon and Philips[5] carefully examined the IR spectra of many acetates with known X-ray crystal structures, arriving at the following conclusions: (1) Unidentate complexes (structure **I**) exhibit Δ values ($\nu_{as}(CO_2) - \nu_s(CO_2)$) that are markedly greater than those in the ionic complexes, 164−171 cm^{-1}. (2) Chelating bidentate complexes (structure **II**) and/or bridging complexes (structures **III**, **IV**) exhibit Δ values that are significantly less than those in the ionic complexes.

By extending the complexes from Ge(tpp)(OAc)$_2$ (**9**) and In(tpp)(OAc) (**6**) to metals of groups IIIA and IVA and the porphyrin ligand from tpp to tmpp and tpyp, the complexes M(por)(OAc)$_n$ (n = 1 or 2 and por = tpp, tmpp, and tpyp) were made. Notably, it is extremely difficult to unambiguously assign the bands $\nu_{as}(CO_2)$ and $\nu_s(CO_2)$ for carboxylates of M(por)-(OAc)$_n$ from the IR spectra. The main bonding types can be distinguished by NMR spectra. The total screening constant (σ) for molecules can be written as a sum of the separate terms:[6]

$$\sigma = \sigma_d(\text{local}) + \sigma_p(\text{local}) + \sigma_m + \sigma_r + \sigma_e + \sigma_s$$

where σ_d(local) denotes the local diamagnetic shielding term, σ_p(local) represents the local paramagnetic shielding term, σ_m is the neighboring anisotropy effect, σ_r denotes the effect of

⊗ Abstract published in *Advance ACS Abstracts,* August 1, 1997.

(1) Maskasky, J. E.; Kenney, M. E. *J. Am. Chem. Soc.* **1973**, *95*, 1443.
(2) Cocolios, P.; Guilard, R.; Bayeul, D.; Lecomte, C. *Inorg. Chem*. **1985**, *24*, 2058.
(3) Hong, T. N.; Sheu, Y. H.; Jang, K. W.; Chen, J. H.; Wang, S. S.; Wang, J. C.; Wang, S. L. *Polyhedron* **1996**, *15*, 2647.
(4) Rardin, R. L.; Tolman, W. B.; Lippard, S. J. *New J. Chem*. **1991**, *15*, 417.
(5) Deacon, G. B.; Phillips, R. J. *Coord. Chem. Rev.* **1980**, *33*, 227.
(6) Harris, R. K. *Nuclear Magnetic Resonance Spetroscopy*; Pitman: London, 1983; p 192.

S0020-1669(96)01304-3 CCC: $14.00

Chart 1

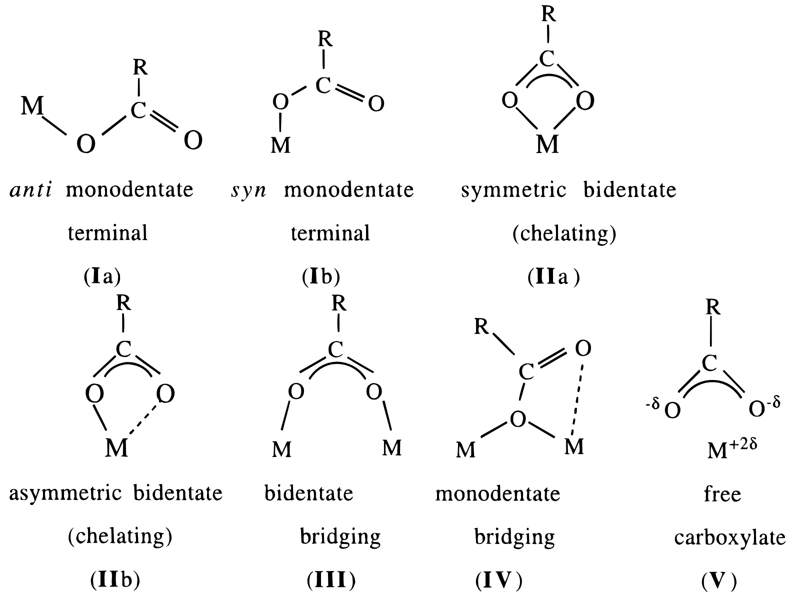

Table 1. ^{13}C Chemical Shift (δ) of Compounds **9**, **9a**, and **9b** in $CDCl_3$ at 24 °C at 75.43 MHz[a,b]

compound	C_α	C_1	$C_{2,6}$	C_β	C_4	$C_{3,5}$	C_{meso}	C*OCH_3	COC*H_3
Ge(tpp)(OAc)$_2$ (**9**)	145.3	140.4	134.3	131.6	128.3	127.0	118.5	166.5	20.6
Ge(tpp)(OAc)(OH) (**9a**)	145.6	140.8	134.4	131.5	128.2	127.0	119.1	166.8	20.2
Ge(tpp)(OH)$_2$ (**9b**)	145.5	141.3	134.7	131.4	128.1	126.9	119.3		

[a] Chemical shifts in ppm relative to the center line of $CDCl_3$ at 77.0 ppm. [b] When water is present in a $CDCl_3$ solution of Ge(tpp)(OAc)$_2$ (**9**), resonances due to Ge(tpp)(OAc)(OH) (**9a**) and Ge(tpp)(OH)$_2$ (**9b**) develop. The contamination peaks (**9a,b**) in the NMR spectrum can be interpreted in terms of the two-stage hydrolysis of compound **9**.

ring currents, σ_e represents the electric field effects, and σ_s is the solvent (or medium) effects. In general, σ_p(local) dominates the chemical shifts of ^{13}C. Karplus and Pople[7] derived the following expression:

$$\sigma_p(\text{local}) = -\frac{e^2\hbar^2}{2m^2c^2}\Delta E^{-1}r_{2p}^{\ -3}(Q_{AA} + \sum Q_{AX})$$

The paramagnetic term increases with a decreasing average electronic excitation energy ΔE and with the inverse cube $r_{2p}^{\ -3}$ of the distance between a 2p electron and the nucleus (A). The above equation also relies on the number of electrons occupying the p orbital (Q_{AA}) and multiple bond contributions (ΣQ_{AX}). These two effects are included in the ($Q_{AA} + \Sigma Q_{AX}$) factor, also known as the charge density and bond order matrix in the MO formalism.[8,9] Hence, the ^{13}C chemical shift depends on the bonding electrons' bond orders (ΣQ_{AX}) and on charge densities. Moreover, the primary effect of charge density on σ_p(local) occurs predominantly through $r_{2p}^{\ -3}$ and, to a lesser extent, through Q_{AA}. The ^{13}C methyl and carbonyl chemical shifts of the acetato group in complexes M(por)(OAc)$_n$ have the potential of identifying the axial binding mode. Importantly, those ^{13}C chemical shifts can be easily measured and assigned, either from the solution or from the solid-state CP/MAS ^{13}C NMR method. A circumstance in which the X-ray data are unavailable suggests that the ^{13}C chemical shift dependence on the axial binding mode is necessary. To our knowledge, for the first time, this work demonstrates this phenomena for diamagnetic metal porphyrin complexes.

(7) Karplus, M.; Pople, J. A. *J. Chem. Phys.* **1963**, *38*, 2803.
(8) Wehrli, F. W.; Marchand, A. P.; Wehrli, S. *Interpretation of Carbon-13 NMR Spectra*, 2nd ed.; Wiley: Singapore, 1989; p 36.
(9) Breitmaier, E.; Voelter, W. *Carbon-13 NMR Spectroscopy*, 3rd ed.; VCH Publishers: New York, 1990; pp 110, 116, 117.

Experimental Section

Preparation of Ge(tpp)(OAc)$_2$ (9). The complex was prepared as described elsewhere.[1] Crystals were grown by diffusing ether vapor into a $CHCl_3$ solution. The complex was dissolved in $CDCl_3$ (99.8% from Aldrich) to yield concentrations of 0.016 M for the ^{1}H NMR and 0.114 M for the ^{13}C NMR measurements. ^{1}H NMR δ (ppm): −1.12 (s, OAc), 7.75 (m, *m*-, *p*-H), 8.17 (m, *o*-H), 9.04 (β-pyrrole H). Table 1 summarizes the ^{13}C NMR data.

Preparation of In(tpp)(OAc) (6). The complex was prepared as described elsewhere.[3] Crystals were grown by diffusing ether vapor into a $CHCl_3$ solution.

IR Spectra. IR spectra of Ge(tpp)(OAc)$_2$ (**9**) were recorded at 24 °C in KBr discs on a Bruker EQUINOX 55 spectrometer.

NMR Spectra. ^{1}H and ^{13}C NMR spectra in $CDCl_3$ were recorded at 300.00 and 75.43 MHz, respectively, on a Varian VXR-300 spectrometer at 24 °C. ^{1}H NMR and ^{13}C NMR are relative to $CDCl_3$ at 7.24 ppm and the center line of $CDCl_3$ at 77.0 ppm, respectively.

The NMR spectra were measured with one pulse sequence. The ^{1}H NMR spectra of **9** were recorded with 64 scans, a 9.0 μs pulse width, a 1.164 s repetition time, a 5500 Hz spectral width, and 12 800 data points. ^{13}C broad-band NMR spectra were recorded with 20 000 scans, a 7.0 μs pulse width (flip angle 40°), a 3.001 s repetition time, a 22 000 Hz spectral width, and 44 032 data points (zero-filled to 81 536). The line broadening factor (LB) was 3 Hz.

Crystallography. Table 2 presents crystal data and other information for Ge(tpp)(OAc)$_2$·2CH_2Cl_2 and In(tpp)(OAc) (**6**). Measurements were taken on a Siemens R3m/V diffractometer using monochromatic Mo Kα radiation (λ = 0.710 73 Å) *via* the $\theta-2\theta$ scan technique. Next, semiempirical absorption corrections were made for Ge(tpp)(OAc)$_2$·2CH_2Cl_2. The structures were then solved by direct methods (SHELXTL PLUS) and refined by full-matrix least squares. All non-hydrogen atoms were refined with anisotropic thermal parameters, where all hydrogen atoms were calculated using a riding model and included in the structure factor calculation. Table 3 lists selected bond distances and angles for both complexes.

Table 2. Crystal Data for Ge(tpp)(OAc)$_2$·2CH$_2$Cl$_2$ and In(tpp)(OAc) (**6**)

emprical formula	$C_{50}H_{38}Cl_4GeN_4O_4$	$C_{46}H_{31}InN_4O_2$
fw	973.2	786.6
space group	$P\bar{1}$	$P2_1/n$
cryst syst	triclinic	monoclinic
cryst color, habit	purple plate	purple plate
a, Å	10.167(2)	10.293(1)
b, Å	11.358(2)	16.601(2)
c, Å	11.672(2)	21.054(2)
α, deg	61.52(1)	
β, deg	74.50(1)	90.28(1)
γ, deg	74.30(1)	
V, Å^3	1125.2(5)	3597.5(5)
Z	1	4
D_{calcd}, g cm^{-3}	1.436	1.452
μ(Mo Kα), cm^{-1}	9.69	7.03
S	1.29	1.14
cryst size, mm^3	0.3 × 0.6 × 0.7	0.3 × 0.5 × 0.5
2θ_{max}, deg	55	50
T, K	293	293
no. of reflns measd	5176	6897
no. of reflns obsd ($F \geq 4\sigma(F)$)	2895	4903
R^a (%)	7.71	3.68
$R_w{}^b$ (%)	9.84	4.87

^{a} $R = [\sum||F_o| - |F_c||/\sum|F_o|]$. ^{b} $R_w = [\sum w(||F_o| - |F_c||)^2/\sum w(|F_o|)^2]^{1/2}$; $w = A/(\sigma^2F_o + BF_o{}^2)$.

Table 3. Selected Bond Distances (Å) and Angles (deg) for Compounds Ge(tpp)(OAc)$_2$·2CH$_2$Cl$_2$ and In(tpp)(OAc) (**6**)

Ge(tpp)(OAc)$_2$·2CH$_2$Cl$_2$			
Distances			
Ge−O(1)	1.874(5)	Ge−N(1)	1.993(7)
O(1)−C(21)	1.18(1)	Ge−N(2)	2.004(5)
C(21)−C(22)	1.51(2)	C(21)−O(2)	1.21(2)
Angles			
Ge−O(1)−C(21)	144.4(9)	O(1)−Ge−N(1)	89.9(3)
O(1)−C(21)−C(22)	119(1)	O(1)−Ge−N(2)	89.4(2)
O(1)−C(21)−O(2)	117(1)	N(1)−Ge−N(2)	89.8(2)
C(22)−C(21)−O(2)	124(1)	N(1)−Ge−N(1a)	180.0(1)
		N(1)−Ge−N(2a)	90.2(2)
In(tpp)(OAc)			
Distances			
In−O(1)	2.322(4)	In−N(1)	2.178(3)
In−O(2)	2.215(4)	In−N(2)	2.174(3)
O(1)−C(21)	1.208(6)	In−N(3)	2.172(3)
O(2)−C(21)	1.205(6)	In−N(4)	2.167(3)
C(21)−C(22)	1.508(6)		
Angles			
In−O(1)−C(21)	90.9(3)	N(1)−In−N(2)	84.7(1)
In−O(2)−C(21)	96.2(3)	N(1)−In−N(3)	144.4(1)
O(1)−C(21)−O(2)	118.5(4)	N(1)−In−N(4)	83.8(1)
O(1)−C(21)−C(22)	120.8(4)	N(2)−In−N(3)	84.0(1)
O(2)−C(21)−C(22)	120.7(4)	N(2)−In−N(4)	143.3(1)
O(1)−In−O(2)	54.4(2)	N(3)−In−N(4)	85.4(1)
O(1)−In−N(1)	126.0(1)	O(2)−In−N(1)	91.7(1)
O(1)−In−N(2)	126.9(2)	O(2)−In−N(2)	87.3(1)
O(1)−In−N(3)	87.1(1)	O(2)−In−N(3)	121.4(1)
O(1)−In−N(4)	87.3(2)	O(2)−In−N(4)	127.7(1)

Results and Discussion

Molecular Structures of Ge(tpp)(OAc)$_2$·2CH$_2$Cl$_2$ and In(tpp)(OAc) (6). Figure 1a,b illustrates the skeletal frameworks of complexes Ge(tpp)(OAc)$_2$·2CH$_2$Cl$_2$, with $P\bar{1}$ symmetry, and In(tpp)(OAc) (**6**), with $P2_1/n$ symmetry. These structures have a six-coordinate germanium or indium atom with four nitrogen atoms of the porphyrinato group and the two monodentate OAc$^-$ ligands or the asymmetric (chelating) bidentate OAc$^-$ ligand for Ge(tpp)(OAc)$_2$·2CH$_2$Cl$_2$ or In(tpp)-

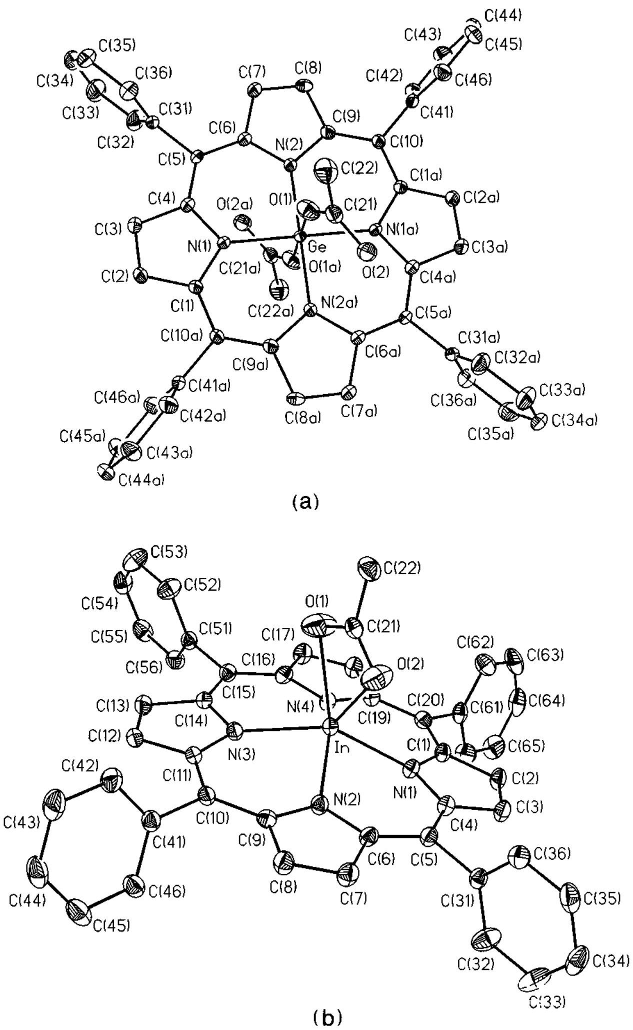

Figure 1. Molecular configuration and atom-labeling scheme for (a) Ge(tpp)(OAc)$_2$·2CH$_2$Cl$_2$ (**9**) and (b) In(tpp)(OAc) (**6**), with ellipsoids drawn at 30% probability. Hydrogen atoms for both compounds and solvents C(71)H(71a)H(71b)Cl(1)Cl(2) for Ge(tpp)(OAc)$_2$·2CH$_2$Cl$_2$ are omitted for clarity. C(21), O(2) of OAc$^-$ in Ge(tpp)(OAc)$_2$·2CH$_2$Cl$_2$ is disordered with an occupancy factor of 0.5 for C(21), O(2) and 0.5 for C(21′), O(2′).

(OAc) (**6**), respectively. Bond distances (Å) are Ge−O(1) = 1.874(5), O(1)−C(21) = 1.18(1), C(21)−O(2) = 1.21(2), and the mean Ge−N = 1.999 Å for Ge(tpp)(OAc)$_2$·2CH$_2$Cl$_2$ and In−O(1) = 2.322(4), In−O(2) = 2.215(4), O(1)−C(21) = 1.208(6), O(2)−C(21) = 1.205(6), C(21)−C(22) = 1.508(6) Å, and the mean In−N = 2.173(3) Å for In(tpp)(OAc) (**6**). The geometry about Ge is an octahedron whereas that around the In^{3+} ion is an approximately square-based pyramid in which the apical site is occupied by an asymmetric (chelating) bidentate OAc$^-$ group. The dihedral angles between the mean plane of the skeleton ($C_{20}N_4$) and the planes of the phenyl group are 83.4° (C(34)) and 103.5° (C(44)) for Ge(tpp)(OAc)$_2$·2CH$_2$Cl$_2$ and 88.7° (C(34)), 84.0° (C(44)), 94.2 (C(54)), and 100.5° (C(64)) for In(tpp)(OAc) (**6**).

The Ge atom lies on the geometrical center (Ct′) of the mean plane of the 24-atom core ($C_{20}N_4$), whereas the indium atom lies 0.674 and 0.762 Å from the four porphyrin nitrogens (4N) and 24-atom porphyrin plane ($C_{20}N_4$), respectively. The central hole's radii (Ct′···N, the distance from the Ct′ to the porphyrinato core N atoms) are 1.999 Å for Ge(tpp)(OAc)$_2$·2CH$_2$Cl$_2$ and 2.069 Å for In(tpp)(OAc) (**6**). Collin and Hoard[10]

(10) Collins, D. M.; Hoard, J. L. *J. Am. Chem. Soc.* **1970**, *92*, 3761.

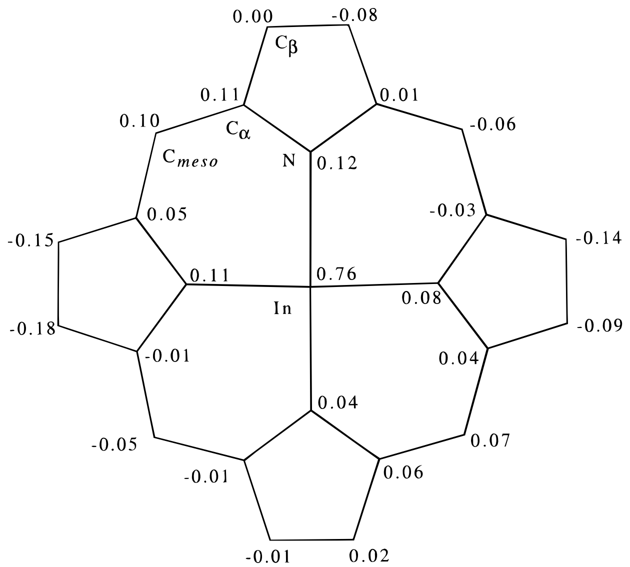

Figure 2. Schematic diagram for the porphyrin core ($C_{20}N_4$ and In) of In(tpp)(OAc) (**6**) in which each atom symbol is replaced by a number showing the displacement (in unit of Å) of that atom from the mean plane of the porphyrin ($C_{20}N_4$) with a typical esd of 0.003 Å.

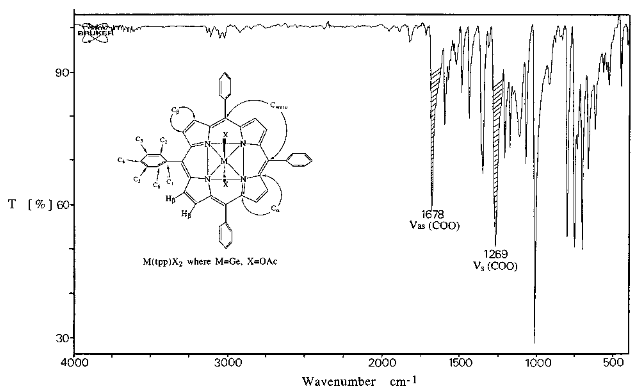

Figure 3. IR spectrum of solid Ge(tpp)(OAc)$_2$ (**9**) at 24 °C. The hatched bands were assigned to the vibrations of the coordinated acetate molecules.

have calculated that the radial strain in the core of a metalloporphyrin is minimized for a “central hole’s radius” of about 2.01 Å. The former is slightly less than 2.01 Å whereas the latter exceeds 2.01 Å. Hence, the Ge(IV) atom is bonded and centered in a slightly contracted porphyrinato core ($C_{20}N_4$) for Ge(tpp)(OAc)$_2$·2CH$_2$Cl$_2$. Meanwhile, the In(III) atom is bonded in a highly expanded porphyrinato core in In(tpp)(OAc) (**6**). The distortion ($C_{20}N_4$ and M) of Ge(tpp)(OAc)$_2$·2CH$_2$Cl$_2$ is “planar” while that of In(tpp)(OAc) (**6**) is “domed”. The net doming is ~0.09 Å (= 0.762 − 0.674) for In(tpp)(OAc) (**6**). Figure 2 depicts the displacement (in Å) of each atom of the porphyrin ($C_{20}N_4$ and In) from the porphyrin mean plane ($C_{20}N_4$) for In(tpp)(OAc) (**6**). As Figure 2 indicates, the average out-of-plane displacements of the In, N, C_α, C_{meso}, and C_β atom are 0.76, 0.09, 0.03, 0.02, and −0.07 Å, respectively.

Infrared Spectroscopy. In Ge(tpp)(OAc)$_2$ (**9**), the interaction of the carboxylate with the germanium is purely unidentate, the second carboxylate oxygen, *i.e.*, O(2), being 3.251 Å from the germanium atom. This finding further confirms the IR spectroscopic method’s effectiveness in assigning a bonding type in metalloporphyrin carboxylates. Figure 3 displays the IR spectrum of Ge(tpp)(OAc)$_2$ (**9**). Figure 4 presents the IR spectrum of dichloro(*meso*-tetraphenylporphyrinato)germanium(IV), Ge(tpp)(Cl)$_2$. Comparing the vibrational frequencies of Ge(tpp)(OAc)$_2$ (**9**) (shown in Figure 3) with those of

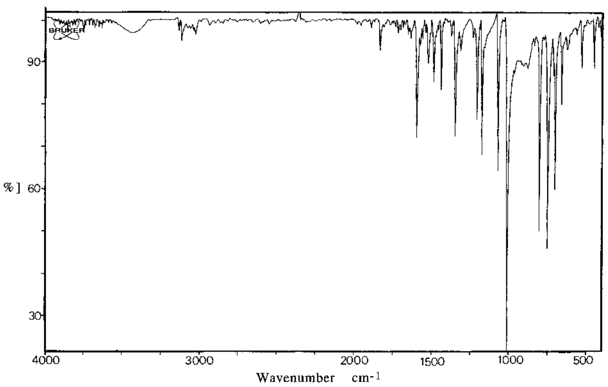

Figure 4. IR spectrum of solid Ge(tpp)Cl$_2$ at 24 °C.

Ge(tpp)(Cl)$_2$ (shown in Figure 4) allows for the bands to be assigned at 1678 (ν_{asym} (CO$_2$)) and 1269 cm^{-1} (ν_{sym} (CO$_2$)). Herein, the frequency difference ($\Delta\nu$) between the asymmetric (ν_{asym}) and symmetric (ν_{sym}) C−O vibrations is 409 cm^{-1}. According to the criterion 1, $\Delta\nu$ values that are significantly greater than those of the ionic complex denote a unidentate formation. In addition, X-ray diffraction analysis unambiguously confirms that Ge(tpp)(OAc)$_2$ (**9**) is a unidentate complex with structure **I**.

According to criterion 2, the frequency difference $\Delta\nu = 141$ cm^{-1} for In(tpp)(OAc) (**6**) excludes monoligation. Nevertheless, it is not feasible to distinguish between a chelating (**II**) or bridging complex (**III**, **IV**) from only the IR data. As X-ray diffraction reveals, In(tpp)(OAc) is an asymmetric (chelating) bidentate complex with structure (**IIb**). Notably, NMR and IR spectroscopies provide complementary methods for investigating the acetate ligand.

NMR Spectroscopy. The acetate’s axial binding in metal porphyrin complexes can alternatively be differentiated by NMR spectra. Table 4 summarizes the NMR, X-ray, and IR data of the acetato group on the complexes M(por)(OAc)$_n$ with $n = 1$ or 2 for the metals IIIA (Ga, In, Tl) and IVA (Ge, Sn) and porphyrin (tpp, tmpp, tpyp). By increasing Δ24 from 0 (for Sn and Ge with planar distortion), 0.46 ± 0.01 (for Ga with domed or MOOP (metal out-of-plane)[11] distortion), and 0.75 ± 0.02 (for In with domed shape) to 0.81 ± 0.07 Å (for Tl with domed shape), the δ(C*H*$_3$) shifts from −1.07 ± 0.07, −0.68 ± 0.05, and −0.08 ± 0.03 to −0.01 ± 0.07 ppm for the complexes M(por)(OAc)$_n$ listed in Table 4. The ring current shielding effect for the ^{1}H resonances of the methyl protons decreases with an increasing distance between methyl protons and C_t'. The above results suggest that as the protons of the acetate ligand are located on a dome with a large Δ24, they move away from the geometrical center (Ct′) of $C_{20}N_4$ for the complexes M(por)(OAc)$_n$. Hence, the shielding of the ring current effect from the 18 π electrons becomes smaller and the ^{1}H chemical shifts are relatively less upfield than those with a small Δ24. According to Table 4, a situation in which the ^{13}C methyl and carbonyl chemical shifts are separately located at 20.5 ± 0.2 (or 18.0 ± 0.7) and 168.2 ± 1.7 (or 175.2 ± 1.6) ppm suggests that the acetate is unidentate (or chelating bidentate) in the complexes M(por)(OAc)$_n$. Exactly why the carbonyl chemical shift is at 168.2 ± 1.7 ppm for unidentate complex **I** remains unclear; however, a downfield shift occurs at 175.2 ± 1.6 ppm for chelating bidentate complex **II**. Nevertheless, this shift may be related to the electronic effect

(11) Prendergast, K.; Spiro, T. G. *J. Am. Chem. Soc.* **1992**, *114*, 3793.

Table 4. NMR, X-ray, and IR Data of the Acetato Group on the M(por)(OAc)$_n$ Complexes with $n = 1, 2$[a]

compound	^{1}H-NMR (ppm) δ(C*H*$_3$)[b]	^{13}C-NMR (ppm) δ(*C*O)	^{13}C-NMR (ppm) δ(*C*H$_3$)	X-ray (Å) $\Delta l = [l_2 - l_1]$ l_1 = M−O	X-ray (Å) l_2 = M−O′(M···O′)	X-ray (Å) Δl[c]	IR (cm^{-1}) $\Delta\nu = [\nu_{as}(COO) - \nu_s(COO)]$ ν_{as}(COO)	IR ν_s(COO)	IR $\Delta\nu$	Δ24 (Å)	carboxylate binding, found	distortion ($C_{20}N_4$ and M)
NaOAc[15,16]	1.91 (s)	184.2	26.2				1578	1414	164[16]		ionic	
Ga(tmpp)(OAc)[17] (**1**)	−0.73 (s)	168.8	20.4	1.869	4.060	2.191	1663	1362	301	0.45	unidentate	domed
In(tmpp)(OAc)[3] (**2**)	−0.11 (s)	176.6[d]	17.4[d]	2.305	2.307	0.002[e]				0.76	symmetric bidentate	domed
		176.0	18.00	2.242	2.339	0.097[e]						
Tl(tmpp)(OAc)[18] (**3**)	−0.07 (d)[d]	173.9[d]	17.7[d]	2.291	2.483	0.192				0.74	asymmetric bidentate	domed
	−0.02 (s)	173.8	18.2									
Sn(tmpp)(OAc)$_2$[17] (**4**)	−1.10	168.5	20.5	2.103	3.351	1.248	1661	1282	379	0	unidentate	planar
Ga(tpp)(OAc)[19] (**5**)	−0.67 (s)[f]	168.8[f]	20.4[f]	1.874	3.021	1.147	1666	1294	372[20]	0.47	unidentate	domed or MOOP
In(tpp)(OAc) (**6**)	−0.05 (s)	176.1	18.1	2.215	2.322	0.107	1562	1421	141[2]	0.76	asymmetric bidentate	domed
Tl(tpp)(OAc)[21,22] (**7**)	0.06 (d)[g]	173.1[h]	18.5[h]	2.299	2.361	0.062	1556	1412	144	0.84	symmetric-bidentate	domed
		174.9[g]	18.8[g]									
Sn(tpp)(OAc)$_2$[23] (**8**)	−1.07 (s)	166.0[h]	20.7[h]	2.086	3.630	1.544	1663	1284	379	0	unidentate	planar
		168.4	20.6									
Ge(tpp)(OAc)$_2$ (**9**)	−1.12 (s)	166.5	20.6	1.874	3.251	1.377	1678	1269	409	0	unidentate	planar
Ga(tpyp)(OAc)[17] (**10**)	−0.63 (s)	169.5	20.5								(unidentate)[i]	
In(tpyp)(OAc)[3] (**11**)	−0.07 (s)	176.8	17.7	2.185	2.412	0.227				0.73	asymmetric bidentate	domed
Tl(tpyp)(OAc)[24,25] (**12**)	−0.05 (d)[g]	174.1[g]	17.6[g]	2.266	2.512	0.246				0.86	asymmetric bidentate	domed
Sn(tpyp)(OAc)$_2$[17] (**13**)	−1.00	168.4	20.5								(unidentate)[i]	

[a] NMR data were recorded in $CDCl_3$ at 24 °C, unless specified; where Δ24 denotes the displacement of the metal center from the plane of the macrocycle atoms ($C_{20}N_4$). [b] Key: s = singlet, d = doublet. [c] Let M−O = l_1, M−O′ (or M···O′) = l_2, and $\Delta l = l_2 - l_1 > 0$. The chelating bidentate binding modes of acetate in the mononuclear complexes, M(por)(OAc)$_n$, may be classified by the following: (i) if $\Delta l \leq 0.1$ Å, the binding mode is symmetric (chelating) bidentate; (ii) if 0.1 Å < Δl, the binding mode is asymmetric (chelating) bidentate. [d] NMR data were recorded in CD_2Cl_2 at −70 °C. [e] Δl = 0.002 Å for In(1)(tmpp)(OAc) and 0.097 Å for In(2)(tmpp)(OAc). [f] NMR data were recorded in CD_2Cl_2 at 24 °C. [g] NMR data were recorded in CD_2Cl_2 at −90 °C. [h] Solid state CP/MAS ^{13}C-NMR at 24 °C. [i] The structure was obtained by a prediction based on the observed ^{13}C chemical shifts of structurally characterized complexes.

of the metal center. The mesomeric structures of complexes of type **Ib** can be expressed as follows:

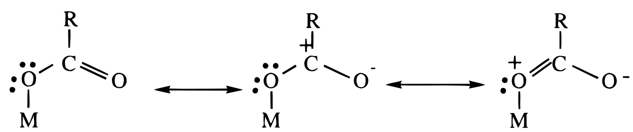

(**I**b) (**I**b′) (**I**b″)

The downfield shifting of +7 ppm for a complex with structure **II** relative to structure **I** can be readily interpreted in terms of an increased polarization of the carbonyl bond, as represented by **IIb** and **IIa**. This phenomenon closely resembles the structure of **Ib′**, except that structure **II** (chelating bidentate) has one more metal−oxygen bond. Consequently, the carbonyl carbon in **II** becomes more positive, thereby accounting for why deshielding occurs. This deshielding effect can be explained in that decreasing the electron density at the carbonyl carbon atom tends to contract the 2p orbitals and, subsequently, causes r_{2p}^{-3} to increase. In a similar manner, intramolecular hydrogen bonds cause the downfield shifts of +6.2 and +8.4 ppm for salicylaldehyde and *o*-hydroxyacetophenone relative to the parent compounds.[9,12] The methyl carbons appear at 18.0 ± 0.7 ppm in structure **II**; however, those carbons are slightly shifted to a lower field, *i.e.*, 20.5 ± 0.2 ppm, in structure **I**. The downfield shift of ∼2.5 ppm for the methyl carbons might originate from the neighboring anisotropic deshielding effect (σ_m) of the more localized carbonyl group (C═O) in structure **I**. This shift correlates with the expected ∼2 ppm for a maximum effect of σ_m. Applying the above criteria to the new complexes Ga(tpyp)(OAc) and Sn(tpyp)(OAc)$_2$ would allow us to predict that the acetate bonding to the metals (Ga, Sn) is unidentate. The upfield shifts for the ^{1}H resonances of the acetato ligand is due to the ring current effects, *i.e.*, $\sigma \approx \sigma_r$. Notably, the ring current effects seldom exceed 10 ppm for ^{1}H NMR[13] and 2 ppm for ^{13}C NMR.[9] Hence, the ring current contribution is relatively less important in determining the ^{13}C chemical shifts than proton shifts.[14] Interestingly, the metal center's large electronic effect dominates the anisotropic ring current effect of the (distorted) π-system in the case of the carbon shifts, *i.e.*, $\sigma \approx \sigma_p$(local). Such domination accounts for why the ^{13}C methyl and carbonyl chemical shifts are independent of the amount of doming, as compared to the dependence of the ^{1}H chemical shifts on the amount of doming.

Conclusions

This work applies, for the first time, the ^{13}C chemical shifts to diagnose the carboxylate coordination. The two correlations

(12) Stothers, J. B. *Carbon-13 NMR Spectroscopy*; Academic Press: New York, 1972; p 287.
(13) Cheng, P. C.; Liu, I. C.; Hong, T. N.; Chen, J. H.; Wang, S. S.; Wang, S. L.; Lin, J. C. *Polyhedron* **1996**, *15*, 2733.
(14) Becker, E. D. *High Resolution NMR*, 2nd ed.; Academic Press: New York, 1980; p 76.
(15) Pouchert, C. J.; Behnke, J. *The Aldrich Library of ^{13}C and ^{1}H FT NMR Spectra*, 1st ed.; Aldrich: Milwaukee, WI, 1993; Vol. I, p 849(A).
(16) Ito, K.; Bernstein, H. J. *Can. J. Chem.* **1956**, *34*, 170.
(17) Hong. T. N.; Sheu, Y. H.; Chen, J. H. Unpublished results.
(18) Sheu, Y. H.; Hong, T. N.; Lin, C. C.; Chen, J. H.; Wang, S. S. *Polyhedron* **1997**, *16*, 681.
(19) Hsieh, Y. Y.; Sheu, Y. H.; Liu, I. C.; Lin, C. C.; Chen, J. H.; Wang, S. S.; Lin, H. J. *J. Chem. Crystallogr.* **1996**, 26, 203.
(20) Kadish, K. M.; Cornillon, J. L.; Coutsoles, A.; Guilard, R. *Inorg. Chem.* **1987**, *26*, 4167.
(21) Chen, J. C; Jang, H. S.; Chen, J. H.; Hwang, L. P. *Polyhedron* **1991**, *10*, 2069.
(22) Suen, S. C.; Lee, W. B.; Hong, F. E.; Jong, T. T.; Chen, J. H.; Hwang, L. P. *Polyhedron* **1992**, *11*, 3025.
(23) Liu, I. C.; Lin, C. C.; Chen, J. H.; Wang, S. S. *Polyhedron* **1996**, *15*, 459.
(24) Fuh, J. J.; Tang, S. S.; Lin, Y. H.; Chen, J. H.; Liu, T. S.; Wang, S. S.; Lin, J. C. *Polyhedron* **1994**, *13*, 3031.
(25) Tang, S. S.; Lin, Y. H.; Sheu, M. T.; Lin, C. C.; Chen, J. H.; Wang, S. S. *Polyhedron* **1995**, *14*, 1241.

proposed herein might be valid for diamagnetic metal porphyrin complexes.

Acknowledgment. The authors would like to thank the National Science Council of the Republic of China for financially supporting this work under Contract No. NSC 86-2113-M-005-008. Dr. Chu-Chieh Lin (National Chung-Hsing University) is thanked for taking the single-crystal X-ray measurements.

Supporting Information Available: Tables of structure determination summary, atomic coordinates, bond lengths, bond angles, anisotropic displacement, and H-atom coordinates coefficients and ORTEP diagrams for compounds **6** and **9** (21 pages). X-ray crystallographic files, in CIF format, for compounds **6** and **9** are also available on the Internet. Ordering and access information is given on any current masthead page.

IC961304I